Incorporating Spatio-Temporal Changes of Well Irrigation into a Distributed Hydrologic Model to Improve Groundwater Anomaly Estimations for Basins with Expanding Agricultural Lands

Cihangir Koycegiz[1] · Mehmet Cuneyd Demirel[2] · Omer Lutfi Sen[3] ·
Meral Buyukyildiz[1]

Abstract

This paper seeks to address the deficiency of utilizing satellite-based GRACE observations and model-based GLDAS water budget components in estimating the changes in the groundwater storage in Konya Endorheic Basin (KEB), a basin experiencing considerable land use land cover (LULC) change, primarily agricultural expansion. Cereal cultivation in the basin has a slight decreasing trend, however, the cultivation of crops with high water consumption, such as maize and sunflower, is increasing substantially. And total agricultural areas are increasing. GRACE-GLDAS approach does not accurately give the long-term groundwater decline in the basin, mainly because the land surface models employed in GLDAS cannot realistically simulate variations in water budget components as they do not consider the changes in LULC and do not possess an elaborated irrigation scheme. Here, we used a fully-distributed mesoscale hydrologic model, mHM, that can handle multiple LULC maps from different years. The model was modified to incorporate the spatio-temporal changes of agricultural fields in KEB and an explicit irrigation scheme since we hypothesized that the groundwater depletion is mainly caused by well irrigation. mHM was calibrated against streamflow observations for the period 2004–2019. The simulations show that the use of mHM with the incorporated features gives groundwater storage changes that are more consistent with the well-based observations than those obtained from the GRACE-GLDAS approach. On the other hand, the mHM simulation with a static LULC map, as in GLDAS models but with a better representation of irrigated fields, provides groundwater anomaly changes that are more consistent with the GRACE-GLDAS results, a further justification of insufficiency of the GLDAS-based approach in estimating groundwater variations for basins with considerable landscape change.

Extended author information available on the last page of the article

1 Introduction

Endorheic basins account for almost one-fifth of the Earth's land surface, and about half of the regions experiencing water stress (Wang et al. 2018). The endorheic basins have a water balance in which the surface flow cannot overcome the topographical barriers and the effect of evapotranspiration is usually strong. In addition to their sensitive hydrology, the water demand has been increasing with time with the rising population in these basins. Considering the impact of climate change, endorheic basins are at the forefront of the basins that experience significant water stress (Wada et al. 2011). The increase in human impacts on the world's surface has increased the drought effects and groundwater consumption in the basins (Rodell et al. 2018; Cavus et al. 2022). Human water consumption has increased the frequency of global drought by 27% and its severity by 10–500% (Wada et al. 2013).

The land use/cover change (LULC) is one of the most important human impacts, influencing the hydrological cycle on global as well as local scales. Anthropogenic effects such as changes in carbon emissions due to industrialization and urbanization also affect the hydrological cycle parameters (Jiongxin 2005). Groundwater resources are exposed to excessive use due to insufficient surface water resources in arid regions. This situation leads to the extinction of the flora as a result of insufficient water intake, and then to a decrease in fauna due to problems in the nutrient supply. This chain of cause and effect has an adverse effect on human lives. Improper agricultural practices to meet human needs cause inefficient use of freshwater resources (Wu et al. 2013).

Deforestation, desertification, and agricultural activities that are not planned with sustainable strategies are at the forefront of the LULC change that negatively affects the hydrological cycle. Therefore, LULC is an important parameter in the management of water resources (Findell et al. 2017). Improper agriculture leads to rapid depletion of water resources as well as low productivity. With the spread of agricultural activities and urbanization, forest areas are rapidly being destroyed. Forests prevent the rapid outflow of water coming in through precipitation. In addition, they contribute to the persistence of precipitation in the region where they are located. In deforested land, precipitation will quickly turn into surface runoff, and water resources will be more difficult to manage. The severity and frequency of floods also increase depending on the increase in surface flow (Al-Masnay et al. 2022; Al-Aizari et al. 2022, 2024). Drylands cover 41% of the Earth's land surface and 45% of the world's agricultural land. These arid areas are regions where human impact is intense and where the effects of climate change are strongly manifested (Burrell et al. 2020).

Gravity Recovery and Climate Experiment (GRACE) and Global Land Data Assimilation System (GLDAS) are frequently used to observe global hydrometeorological changes under human and climatic effects. The GRACE satellite, which observes total water storage (TWS) anomalies, allows the hydrological cycle to be examined as a whole, globally, and regionally (Save et al. 2016; Wiese et al. 2016; Nemati et al. 2020). With the information obtained from the GRACE and GLDAS data, research is also carried out on changes in the global water budget and groundwater resources (Brookfield et al. 2018; Long et al. 2016; Soni and Seyd 2015; Tregoning et al. 2012).

It is stated that the groundwater anomalies obtained from GRACE and GLDAS data in some parts of the world are inconsistent with the in-situ well measurement data (Brookfield et al. 2018). Ali et al. (2022) compared GRACE-GLDAS-based groundwater anomalies with in-situ well data in the highly irrigated Indus basin, the majority of which is located

in Pakistan. They found that the magnitude of the estimated trend was not consistent with that of in situ observations (a decreasing trend of 3–4 mm/yr), although the direction of the trends was the same. The low resolution of GRACE and anthropogenic effects were cited as reasons for the discrepancy. Amiri et al. (2023) evaluated GRACE-GLDAS-based groundwater storage (GWS) anomalies with in-situ well data in Yazd province, Iran, where groundwater is used extensively. They also found that, while the decreasing trend direction is consistent, there is no consistency in terms of magnitude. They attributed this discrepancy to the non-uniform distribution of the in-situ wells. Rusli et al. (2023) combined hydrological and groundwater flow models with GRACE satellite observation data to observe the groundwater anomaly in the data-scarce Bandung basin in Indonesia for the 2005–2015 period. They noted that the missing GRACE data and local time-lags might cause bias in the water budget estimates. Shen et al. (2015) investigated groundwater anomalies in the highly irrigated Hai River basin in northern China. They found inconsistency between the trend of in situ well observations, reaching -83.8 mm/yr, and that of the GRACE-based GWS anomaly, estimated as -17 mm/yr. Similar inconsistencies were reported for the California Central Valley, Mississippi Basin, and Bangladesh (Scanlon et al. 2012).

This study is the first comprehensive study incorporating land cover change into a hydrological model to address the inconsistent groundwater anomaly trends estimated by the GRACE-GLDAS approach. The novelty of this study lies in proposing a robust hydrologic model-based framework for groundwater analysis in irrigated endorheic basins after analyzing the overlooked issue of GLDAS data in groundwater depletion analysis as stated in the literature. The objectives of this study are (i) to modify the physically-based fully-distributed hydrological model, mHM, to incorporate an irrigation scheme and temporal evolution of land cover change, (ii) to calibrate the hydrological model against streamflow observations, (iii) to examine the temporal and spatial variation of evapotranspiration, (iv) to comparatively analyze the groundwater anomaly changes obtained from in-situ well observations and different approaches including the GRACE-GLDAS.

2 Study Area

KEB is located in the Anatolian Plateau, between 36°51'−39°29' North and 31°36'−34°52' East coordinates, with a karstic formation (Fig. 1). The altitude in the basin varies between 850 and 3450 m. Its climate is characterized as continental. Annual precipitation varies between 280 and 1000 mm. Average annual precipitation in the basin is about 400 mm. South of the basin, as elevation increases with the Taurus Mountain range, forest areas become common, while agriculture is carried out intensively in the low-altitude plains (Gokmen et al. 2013). Several water resources control structures have been built in the basin in the last 20 years (KOP 2016). Furthermore, developing agricultural technology and food demand of increasing population have caused rapid expansion of agriculture. Although the limited surface water resources are used extensively in agricultural activities, main water resources remain to be the groundwater systems (Koycegiz et al. 2023).

The KEB spatially averaged monthly Leaf Area Index (LAI) time series, obtained from the MODIS dataset for the period 2004–2019 (Table 1), shows an increasing trend (Figure S1a). The distribution of LAI in May with the highest values for the years 2004, 2006, 2009, 2011, 2013, 2015, and 2019 clearly indicates that the basin is getting greener with agricul-
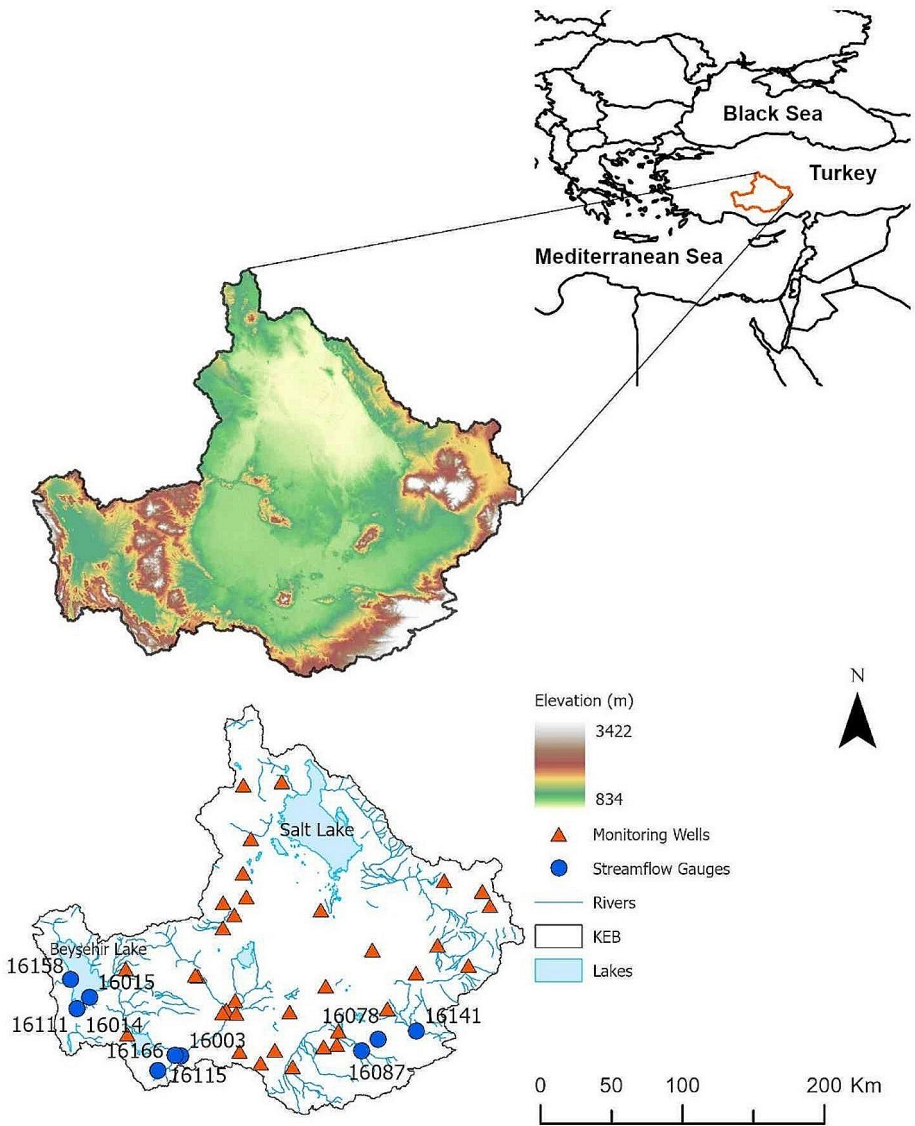
Fig. 1 Map of the Konya Endorheic Basin (KEB) with the locations of the streamflow gauges and monitoring wells

tural activities, although there are interannual variations most likely because of precipitation alterations (Figure S1b).

3 Data

Table 1 gives information about the datasets used in this study. GRACE-RL06 TWSA data was obtained from the mass concentration (mascon) solutions produced at the National Aeronautics and Space Administration (NASA)'s Jet Propulsion Laboratory (JPL) processing centers (Wiese et al. 2016) and the University of Texas Space Research Center (CSR) in Austin (Save et al. 2016). Its spatial resolution is 0.5°×0.5°; the temporal resolution is monthly. The time series data obtained by averaging the JPL and CSR data covers the period from August 2002 to December 2019. We utilized precipitation, soil moisture, canopy water, snow water equivalent, surface water, and evapotranspiration data from GLDAS (GLDAS 2.1; Rodell et al. 2004), with a spatial resolution of 0.25°×0.25°, and a temporal resolution of monthly.

Table 1 Information about the datasets used in the study

Variable	Product/Source	Temporal Resolution	Spatial Resolution
Terrestrial Water Storage Anomaly (TWSA)	GRACE mascon solutions (CSR)	Monthly	0.50°
Terrestrial Water Storage Anomaly (TWSA)	GRACE mascon solutions (JPL)	Monthly	0.50°
Soil Moisture Storage (SMS)	GLDAS	Monthly	0.25°
Canopy Water Storage (CWS)	GLDAS	Monthly	0.25°
Snow Water Equivalent (SWE)	GLDAS	Monthly	0.25°
Surface Water Storage (SWS)	GLDAS	Monthly	0.25°
Evapotranspiration	GLDAS	Monthly	0.25°
Precipitation	ERA5	Daily	0.25°
Average Temperature	ERA5	Daily	0.25°
Groundwater Level (GWL)	GDSHW	Monthly	Point
Streamflow	GDSHW	Monthly	Point
Land Use/Cover (LULC)	MODIS	Annual	0.001953125°
Leaf Area Index (LAI)	GIMMS	Monthly	0.001953125°
Leaf Area Index (LAI)	MODIS	Monthly	0.001953125°
Digital Elevation Model (DEM)	SRTM	-	0.001953125°
Cultivated Areas of Crops	TURKSTAT	Annual	-
Crop Yields	TURKSTAT	Annual	-

Daily total precipitation and daily average temperature data used as spatially distributed hydrological model input were obtained from European Center for Medium-Term Weather Forecasts (ECMWF) Reanalysis v5 (ERA5) (ECMWF 2021). Its spatial resolution is 0.25°×0.25°. Monthly groundwater level and streamflow data were obtained from the General Directorate of State Hydraulic Works (GDSHW) of Türkiye. In-situ well measurements were converted to groundwater level with specific yields defined for the basin (Koycegiz et al. 2023). The locations of streamflow gauges and in-situ wells are given in Fig. 1.

The annual LULC data were obtained from Moderate Resolution Imaging Spectroradiometer (MODIS) datasets. The LAI used as input to the hydrological model was obtained monthly from the Advanced Very High Resolution Radiometer (AVHRR) Global Inventory Modeling and Mapping Studies (GIMMS) data set. The spatial resolution of both LULC and LAI data is 0.001953125°. The Digital Elevation Model (DEM), which was required during the preparation of the inputs of the hydrological model run, was obtained from the Shuttle Radar Topography Mission (SRTM), with a spatial resolution of 0.001953125°. The cultivated areas and crop yields of different products were obtained from TURKSTAT. The data for cereals (barley, wheat, rye), sugar beet, maize, melon, watermelon, sunflower, pumpkin and potato are provided annually.

4 Methodology

Figure 2 shows the workflow diagram of the study including the incorporation of the irrigation processes into mHM, estimation of uniform irrigation (see Supplementary Materials S2.3 and S2.4 for details), and the five scenarios involving GRACE, GLDAS and mHM (see Table S2 for details). The GRACE-GLDAS based groundwater anomaly methodology and performance metrics used in this study are provided in the Supplementary Materials S2.1 and S2.5, respectively.

4.1 Mesoscale Hydrologic Model (mHM)

In this study, we utilized the open-source, fully-distributed hydrological model, mHM. The physically-based mHM makes calculations with the finite element method (Samaniego et al. 2018). The main feature that distinguishes mHM from other fully-distributed hydrological models is that each year's LULC data can be introduced into the model as input (Ergün and Demirel 2023). Thus, more consistent results can be obtained in water budget calculations in regions where the land cover changes over time. More accurate evapotranspiration outputs can be obtained by correcting the potential evapotranspiration (PET), a meteorological input of mHM, with the LAI and aspect maps. In this way, mHM can effectively adapt to the wilting and growth dynamics of plants. Hydrological models have difficulty producing accurate results for the soil moisture zone. While the surface cover of the basin dynamically affects soil moisture, groundwater storage is in a hydrological relationship with the soil moisture zone. Feddes et al. (1976) and Jarvis (1989) equations are used to calculate soil moisture, root water intake, and evaporation in mHM. Four different application options developed based on these equations are available in mHM (Demirel et al. 2018).

Dynamically Dimensioned Search (DDS) algorithm was preferred in the mHM calibration phase. DDS algorithm produces very effective results in calibrating physically based
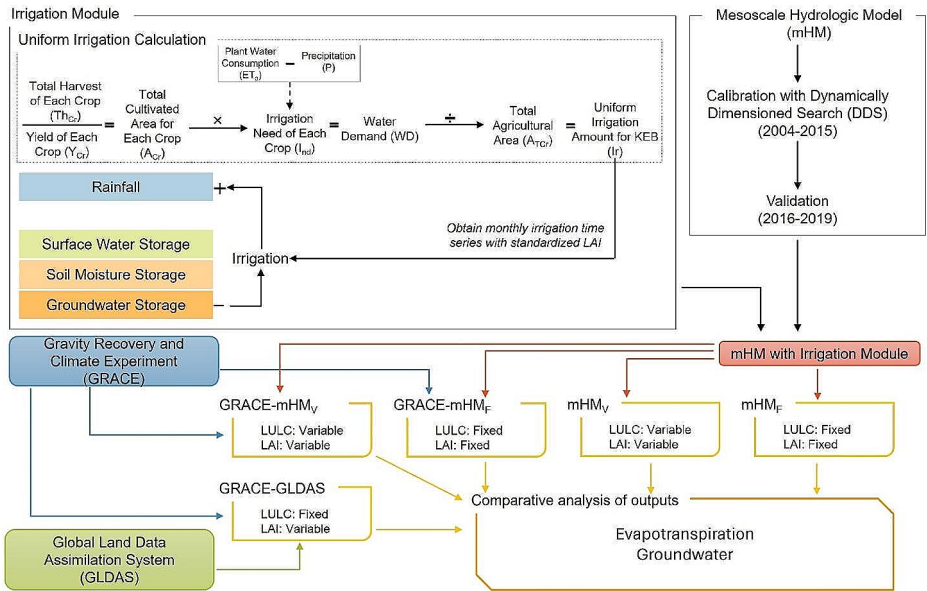
Fig. 2 Workflow diagram of the study providing with the details of the irrigation module incorporated into mHM, calibration of the model and groundwater anomaly estimations involving one or more of the GRACE, GLDAS and mHM data

models (Lespinas et al. 2018). It is stated that DDS achieves successful results in convergence problems to a good solution (Tolson and Shoemaker 2007). Behrangi et al. (2008) stated that DDS can produce successful results, especially in calibrating models that require compelling computation. In this study, the 2002–2003 warm-up period, 2004–2015 calibration, and 2016–2019 validation period were evaluated. The Kling-Gupta Efficiency (KGE) (Gupta et al. 2009) performance metric was preferred as the objective function.

4.2 Integrating the Irrigation Process into the mHM

Limited surface water resources in KEB force farmers to use subsurface water resources for irrigation purposes. To integrate irrigation information into the hydrological processes simulated by the calibrated mHM, the irrigation amount per grid determined for KEB was added to precipitation. The groundwater anomalies were then updated by subtracting the irrigation amount from the previous groundwater anomalies.

Total irrigation water requirement was determined depending on annual yields of cereals (barley, wheat, and rye), maize, sugar beet, melon, watermelon, sunflower, potato, and pumpkin which are the main agricultural products of KEB. Table S1 presents the plant water consumptions of the main agricultural products in KEB. The irrigation amount, which changes depending on the annual yield values and amount of precipitation, is added to the modeled precipitation in accordance with the resolution of the grids (0.25°) in the meteorology layer of mHM. Details of the irrigation module are given in Supplementary Materials S2.3.

4.3 LULC Scenarios

We considered five different LULC change scenarios to observe the hydrological effects (Fig. 2 and Table S2). The first two scenarios were simulated with mHM. In mHM$_F$, the model (mHM) was configured to include a fixed LULC map and long-term monthly averaged LAI, while in mHM$_V$ it included annually varying LULC and monthly varying LAI. In the simulations involving these two scenarios, groundwater storage anomaly (GWSA) was calculated directly from the mHM outputs. The GRACE-GLDAS scenario was constructed with the help of GRACE and GLDAS datasets. It should be noted that the GLDAS models use fixed LULC and monthly changing LAI. The GRACE-mHM$_F$ and GRACE-mHM$_V$ used the simulations from the mHM$_F$ and mHM$_V$, respectively. However, GWSA was calculated by considering the GRACE-based total water storage anomaly (TWSA), as in the GRACE-GLDAS scenario but it involved mHM outputs instead of GLDAS outputs.

5 Results

5.1 Performance of mHM in Simulating Streamflow

The streamflow performance of mHM for two scenarios (mHM$_F$ and mHM$_V$) is shown through the time series and radar graphs utilizing data from the 10 streamflow gauges (Figure S5 and Fig. 3, respectively). The months with missing observational data are excluded from the performance evaluation. In general, mHM simulates the streamflow in all stations fairly well, but both underestimations (e.g., at 16015) and overestimations (e.g., at 16014, 16111) are also evident. The model is also able to successfully simulate the impact of
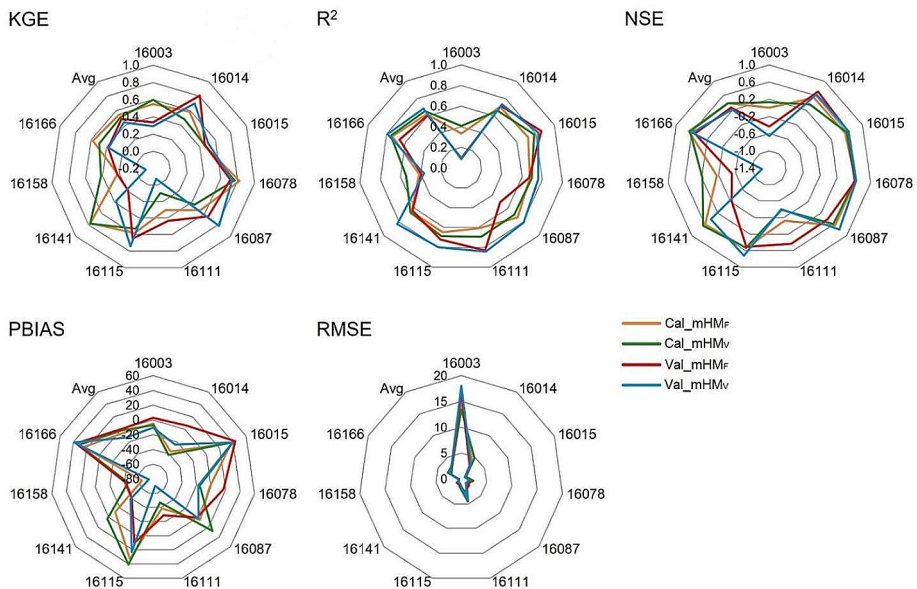

Fig. 3 Performance results of mHM streamflow estimations for both calibration and validation periods

2007–2008 drought on streamflow at most stations. The radar graphs (Fig. 3) show similar and satisfactory performance for the mHM$_F$ and mHM$_V$ simulations across various metrics. Scatter plots related to mHM flow estimation results and a table of performance metrics are given in Figure S4 and Table S3, respectively.

5.2 Harvested Areas and Irrigation of KEB Major Crops

Figure 4 illustrate the harvested areas of KEB's major products and the amount of irrigation, respectively (TURKSTAT 2022). The KEB agricultural lands have increased significantly (Fig. 4). It should be noted that cereals occupy the most space in agriculture of KEB. However, it shows a decreasing trend. There is a remarkable increase in maize-cultivated areas. The drought experienced in 2007–2008 also affected the agricultural activities throughout the basin. There is usually a decrease in the harvested areas in these years. Along with maize, sunflower, melon, and watermelon are among the agricultural products whose cultivated areas have increased in recent years. The areas for sugar beet, pumpkin, and potato show an increasing trend over the study period, albeit with some yearly variations.

Uniform irrigation load time series on the total agricultural land of KEB major crops shows that, after the drought of 2007–2008, the amount of irrigation in the basin has increased significantly (Fig. 4). During the drought, although there was no significant change in agri-
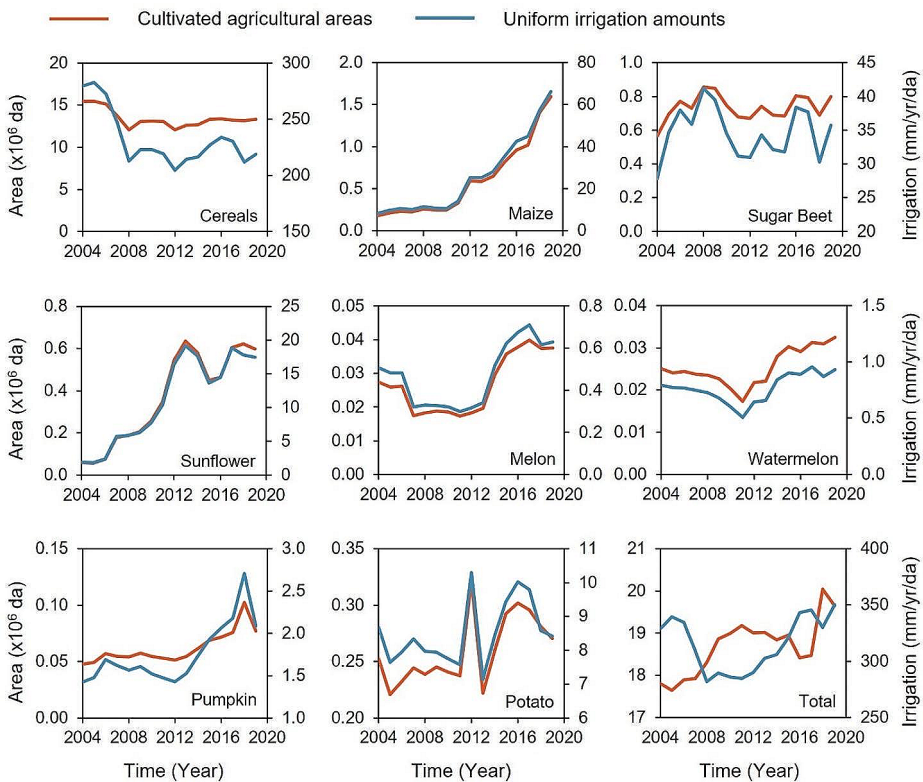

Fig. 4 Cultivated agricultural areas and uniform irrigation amounts on the total agricultural area for different crops in KEB

cultural areas, there was a sudden decrease in the amount of irrigation. While there wasn't a significant change in the amount of irrigation until 2012, a significant increase was observed in the agricultural areas, which could be due to an increase in dry farming. Subsequently, the amount of irrigation shows a significant increasing trend. This strong upward trend seems to be unaffected by the reduction of agricultural land towards the year 2016, which could be due to the preference for irrigated agriculture in dry farming areas and the preference for products that demand more water instead of products that demand less water. It should be noted that the water allocation of cereals is gradually decreasing, while irrigation for maize, sunflower, pumpkin, melon, and watermelon shows a strong increasing trend, especially during recent years. Although the total irrigation shows a general increasing behavior over the second half of the period, water allocation for sugar beet and potato does not illustrate a clear increasing or decreasing trend.

5.3 Evapotranspiration

The violin graphs of the actual and potential evapotranspiration values are given in Fig. 5. It seems that both the distribution and mean of the simulated aET values in mHM_F and mHM_V are very similar to each other while they are substantially different from those of the GLDAS aET values. The mean of the GLDAS aET data is approximately 15 mm lower. Also, the base of the violin graph of GLDAS shows a lower height stack compared to those of the mHM_F and mHM_V simulations (Fig. 5a). PET provides information about the atmospheric demand for water vapor. In mHM_F, the highest PET estimations show an agglomeration of around 300 mm and the lowest estimations around 60 mm. In mHM_V, it is seen that the highest values are accumulated around 260 mm and the lowest values around 50 mm. The PET averages are 158.09 mm and 145.07 mm for mHM_F and mHM_V, respectively (Fig. 5b). For further insight, the long-term variations of aET and PET for the KEB given in Figures S6-S9 could be examined.

In general, the higher aET estimations of the mHM simulations come from the incorporation of irrigation into the model. Although the GLDAS models can simulate the irrigation processes, the LULC map they used, belonging to earlier years, does not adequately reflect the present time irrigation crop distribution in the basin. In general, climatic trends are observed in both mHM and GLDAS estimations. The mHM_V simulation indicates a bigger trend than both mHM_F simulation and GLDAS data, and this is most likely a result of the inclusion of a yearly varying LULC into the model (Figure S7).

Figures 5c and 5d exhibit the annual total aET time series and monthly distribution of long-term averaged aET for a point (32.84375°E, 38.09375°N) where agriculture is intense. GLDAS has very low aET values (mostly < 500 mm), which is most likely related to the inconsistent LULC assignment for that grid (i.e., a LULC class other than irrigated crop). More realistic aET estimates are made in the scenario in which the LULC is variable (mHM_V). The scenario in which the LULC is fixed (mHM_F) also provides realistic estimates for an irrigated grid. The difference between these two mHM simulations occurs because the LAI values are larger in the mHM_V scenario than in the mHM_F scenario, which is implied by the differences in their seasonal aET variations.

Evapotranspiration is a parameter that is highly variable as spatially. Both mHM_F and mHM_V simulations produce very similar aET patterns to each other (Figure S10). The mHM_V simulation tends to estimate more aET in some areas of the basin, especially in
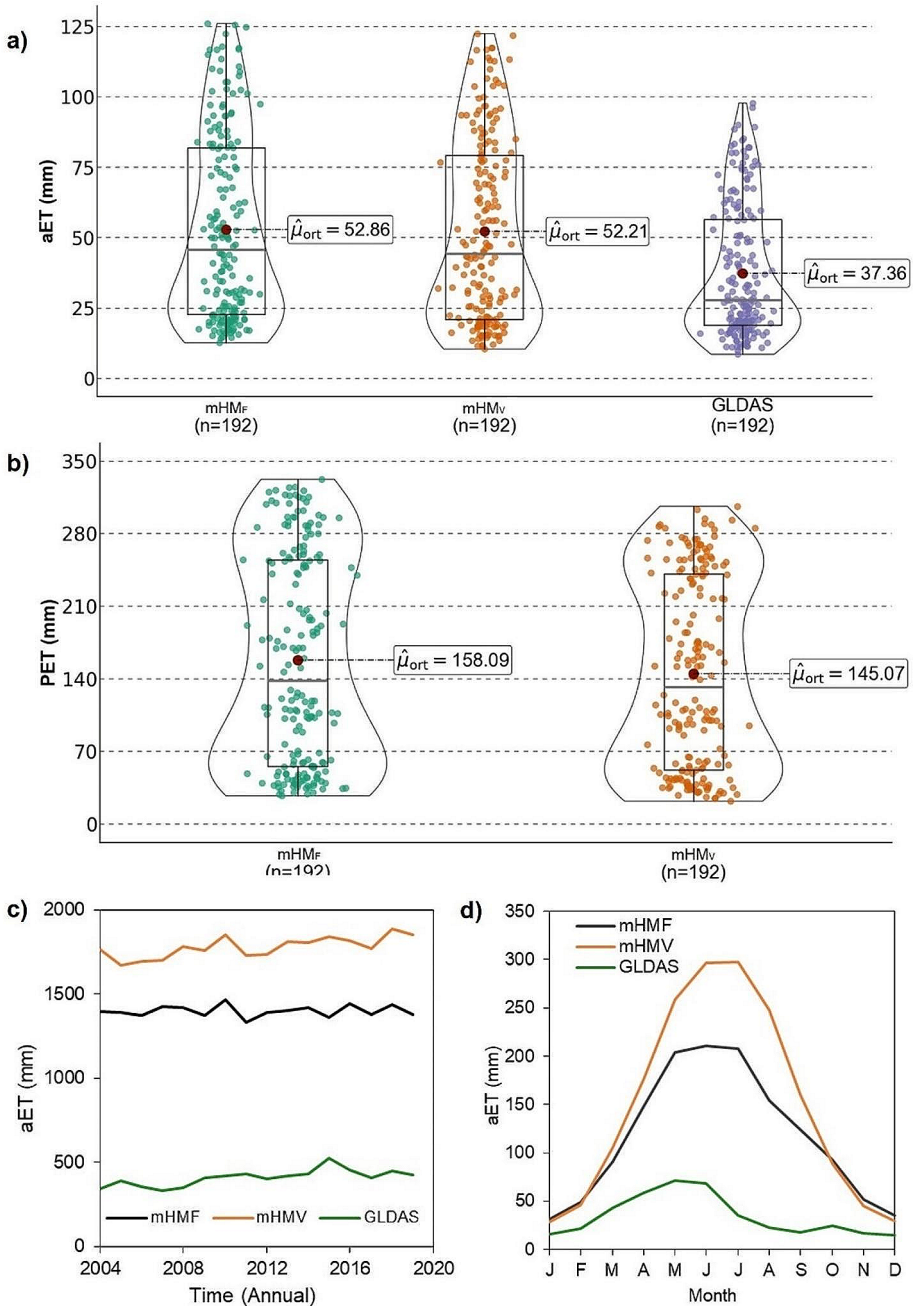
Fig. 5 **(a)** Monthly aET violin plots from mHM_F and mHM_V simulations, and GLDAS data, **(b)** Monthly PET violin plots from mHM_F and mHM_V simulations, **(c)** yearly and **(d)** monthly aET change in an agricultural point in KEB

the agricultural fields where expansion of irrigation is evident. In both simulations, aET is quite high in the middle of the basin (over 1500 mm). It is also larger around Beyşehir Lake. In areas where there is no irrigation, aET could not exceed 500 mm. aET values of 250–750 mm are observed around Salt Lake.

5.4 Groundwater Anomalies

The groundwater level anomaly (GWA) timeseries created using the mHM estimations and GRACE and GLDAS data and those based on in situ measurements are given in Fig. 6. The groundwater observations show a declining trend in groundwater level (GWL). In addition, the drought of 2007–2008 is clearly seen in Fig. 6. The GRACE-GLDAS evaluation does not exhibit a clear declining GWL trend as in the observations. It also shows higher sensitivity to the variations in climate.

It is known that the water drawn from the groundwater storage system by the wells is used in agricultural activities. It seems that the mHM_V simulation represents this process successfully and produces a trend that is in agreement with the observations. Lacking the crucial information about the LULC change in the basin, the mHM_F simulation, however, fails to produce a declining trend consistent with the observations. When we use water budget components estimated by mHM_V, instead of GLDAS, in a GRACE-mHM_V co-evaluation it reveals a more successful GWA estimation than the GRACE-GLDAS co-evaluation. It should also be noted that the GRACE-mHM_F co-evaluation yields a GWA evolution that is very similar to that produced by GRACE-GLDAS co-evaluation, which is an attestation of insufficiency of the latter approach in estimating the long-term changes in the GWA of the basins where LULC change is relatively rapid. Overall, the mHM_V simulation (with $R^2 = 0.840$ and NSE $= 0.822$) performs much better than the others (Figure S11). The results indicate that the inclusion of a variable land cover into the assessments improves the groundwater anomaly estimation.
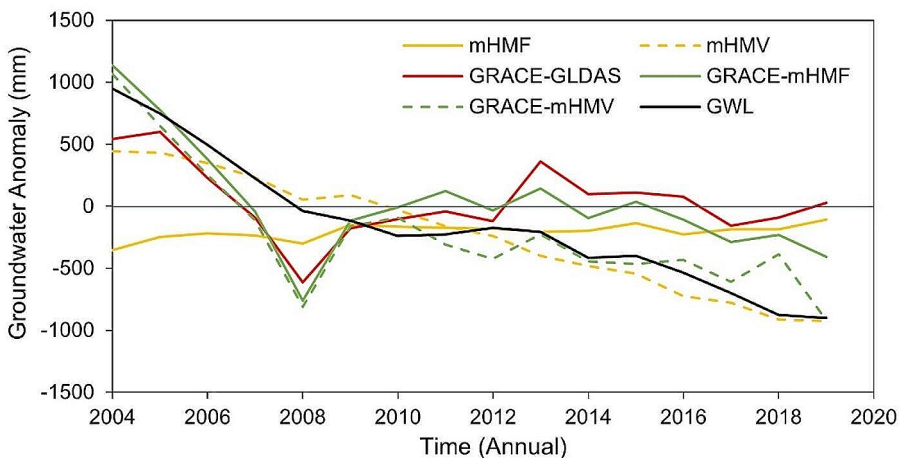

Fig. 6 Annual time series of KEB groundwater level anomalies from five different scenarios (mHM_F, GRACE-mHM_F, mHM_V, GRACE-mHM_V, GRACE-GLDAS) and in-situ observations (GWL)

6 Discussion

The mHM model is a physically-based, spatially distributed model, and its use has advantages and disadvantages. For instance, its ability to run water balance equations by establishing relationships between data sets with different resolutions is an important advantage. Detailed data requirement and high computational cost incurred to simulate the physical processes in detail (Samaniego et al. 2018) are among the disadvantages. The fact that the study area is an endorheic basin with a complex hydrological cycle has led to the need for a comprehensive model such as mHM in this study. The model, used for different basins in Europe, is shown to generally achieve 0.6–0.7 KGE values, which is a sign that it is an acceptable physically-based model in the literature (Rakovec et al. 2016). Thus, the KGE values obtained for the calibration process against the observations from the 10 streamflow stations in KEB stand out to be satisfactory.

This study also explores the consistency in other physical parameters beyond streamflow estimations mostly coming from the stations that are located towards the mountainous parts of the basin, which are not subject to much LULC change. For the large lowland areas, which experience substantial LULC change in the form of agricultural expansion depending on groundwater resources, surface data to calibrate the model lack. For that reason, we choose to evaluate the model performance in terms of its ability to simulate the groundwater anomaly, which could be acquired from the well measurements. It turns out that the use of a static land cover in the model produces inconsistent groundwater anomaly timeseries with the observations, however the incorporation of a realistic land use change into the model, a feature most hydrological models lack, yields more satisfactory results in terms of water budget components for the entire basin. It could be argued that the improvement most likely comes from the improved evapotranspiration estimations in the latter, as it considers the agricultural expansion augmenting the water loss through evapotranspiration. Thus, the use of GLDAS evapotranspiration data in water budget studies for KEB will lead to poor results, as the GLDAS models use static land cover data, which likely causes underestimation of evapotranspiration in the basin. From this point of view, it could be concluded that the changes in surface features are quite important not only for the surface water budget estimations but also for the groundwater anomaly estimations.

The GLDAS dataset is preferred by researchers around the world because of its comprehensive hydrometeorological outputs. The GLDAS-based regional or continental scale assessments may provide consistent results with observations (Rodell et al. 2004). For relatively small areas or basins, however, the role of anthropogenic factors could be quite strong, which cannot be neglected in the modeling. Agricultural activity is one of the anthropogenic factors that significantly affect the hydrological processes. The rapidly changing land cover with agriculture differentiates permeability, evapotranspiration, retention, and convective precipitation events (Findell et al. 2017). Therefore, the surface changes should adequately be represented in the models where they become significant over the time of model integration. The GLDAS data are also readily used together with the GRACE data to estimate groundwater anomalies in different parts of the world (e.g., Long et al. 2016; Soni and Seyd 2015; Tregoning et al. 2012). However, it is stated that this co-evaluation may yield deviations from the observations depending on the surface and subsurface processes in the basins (Brookfield et al. 2018). The present study also presents evidence that the GLDAS and GRACE co-evaluation approach could produce poor results, and therefore

studies involving this approach should first assess the extent of LULC change, especially in basins where the agricultural activities are intense. If it is deemed significant to change the basin-wide hydrological processes, the use of the GLDAS data should be avoided, instead a hydrological model that can handle the surface changes should be run to estimate water budget components that could be substituted for GLDAS data.

KEB is a water-limited basin, and the expansion of agricultural areas and cultivation of crops with high water consumption increase the need for irrigation (Fig. 4). Irrigation need is met from groundwater to a significant extent. Consequently, increased irrigation causes significant reductions in the groundwater storage system.

7 Conclusion

GLDAS data are commonly used together with GRACE TWSA observations to separate the anomalies in groundwater storage from the anomalies in other water storage components in basins. This approach does not provide satisfactory results in basins where land cover change is substantial over time. In this study, we incorporated the land cover change into a hydrological model, mHM, to estimate the anomalies in water storage components in KEB. The results were compared with GLDAS-GRACE based evapotranspiration and groundwater storage anomaly parameters.

Among the major agricultural products, maize and sunflower have a strong increasing trend in the basin. Cereals, the crops with the largest cultivation area, have a decreasing trend. The total agricultural areas in the basin have a strong increasing trend, leading to higher levels of water consumption. Expanding agricultural areas are cultivated with different crops. The amount of irrigation in the basin is very sensitive to climatic changes. It is observed that irrigation decreased significantly during the 2007–2008 drought. However, the amount of irrigation increased rapidly afterward.

The actual evapotranspiration estimations of two mHM simulations (involving a changing land cover in one and a static in the other) with a more realistic irrigation scheme are found to be higher than the GLDAS estimations. Thus, it could be said that the inclusion of land cover change and irrigation information into the hydrological model is crucial to obtain more realistic simulations of basin hydrological processes. The lack of land cover change and irrigation information in GLDAS caused it to contain biased results for evapotranspiration. It is observed that the introduction of an irrigation scheme to the hydrological model, supported by changing land cover information, significantly increases the success of prediction in groundwater storage anomalies. It should be noted that the accuracy of a hydrological model is not only dependent on the calibration of the streamflow parameter but also on the satisfactory representation of anthropogenic processes in basins subject to significant land cover change. The fixed land cover in GLDAS, ignoring anthropogenic changes, seems to be the main reason for the poor performance of the GRACE-GLDAS approach in revealing groundwater depletion in semi-arid KEB. Future work should investigate whether this poor performance of GRACE-GLDAS approach persists in areas with different hydro-climatology.

This study has some limitations, and the relatively coarse resolution of the data used is one of them. A higher spatial resolution would certainly provide more detailed information about the spatial variation of the physical information obtained. In addition, lack of data on

the spatial distribution of statistical data such as cultivated agricultural land and the yield of harvested crops was an issue. The availability of such information would be useful to incorporate the distribution of irrigation into the model.

Authors' Contributions All authors contributed to the study conception and design. C. Koycegiz: Visualisation, Data Collection and Curation, Methodology, Software, Writing-Original draft. M. C. Demirel: Conceptualization, Validation, Writing-Reviewing and Editing, Supervising. O. L. Sen: Conceptualization, Validation, Writing-Reviewing, and Editing, Supervising. M. Buyukyildiz: Writing-Reviewing and Editing, Supervising.

Declarations

Conflict of Interest The authors confirm that there is no conflict of interest.

References

Al-Aizari AR, Al-Masnay YA, Aydda A et al (2022) Assessment Analysis of Flood susceptibility in Tropical Desert Area: a case study of Yemen. Remote Sens 14(16):4050

Al-Aizari AR, Alzahrani H, AlThuwaynee OF et al (2024) Uncertainty reduction in Flood susceptibility mapping using Random Forest and eXtreme Gradient Boosting algorithms in two Tropical Desert cities, Shibam and Marib, Yemen. Remote Sens 16(2):336

Al-Masnay YA, Al-Areeq NM, Ullah K et al (2022) Estimate earth fissure hazard based on machine learning in the Qa' Jahran Basin, Yemen. Sci Rep 12:21936

Ali S, Wang Q, Liu D, Fu Q, Rahaman MM, Faiz MA, Cheema MJM (2022) Estimation of spatio-temporal groundwater storage variations in the Lower Transboundary Indus Basin using GRACE satellite. J Hydrol 605:127315

Amiri V, Ali S, Sohrabi N (2023) Estimating the spatio-temporal assessment of GRACE/GRACE-FO derived groundwater storage depletion and validation with in-situ water quality data (Yazd province, central Iran). J Hydrol 620(A):129416

Behrangi A, Khakbaz B, Vrugt JA, Duan Q, Sorooshian S (2008) Comment on dynamically dimensioned search algorithm for computationally efficient watershed model calibration by Bryan A. Tolson and Christine A. Shoemaker. Water Resour Res 44(12):1–3

Brookfield AE, Hill MC, Rodell M, Loomis BD, Stotler RL, Porter ME, Bohling GC (2018) In situ and GRACE-Based Groundwater observations: similarities, discrepancies, and evaluation in the High Plains Aquifer in Kansas. Water Resour Res 54(10):8034–8044

Burrell AL, Evans JP, De Kauwe MG (2020) Anthropogenic climate change has driven over 5 million km^2 of drylands towards desertification. Nat Commun 11(3853):1–11

Cavus Y, Stahl K, Aksoy H (2022) Revisiting Major Dry Periods by Rolling Time Series Analysis for Human-Water Relevance in Drought. Water Resour Manage 36:2725–2739

Demirel MC, Koch J, Mendiguren G, Stisen S (2018) Spatial pattern oriented Multicriteria Sensitivity Analysis of a distributed hydrologic model. Water 10:1–20

ECMWF (2021) ERA5-Land: Data Documentation. https://confluence.ecmwf.int/display/CKB/ERA5-Land%3A+data+documentation. Accessed on 23 February 2023.

Ergün E, Demirel MC (2023) On the use of distributed hydrologic model for filling large gaps at different parts of the streamflow data. Eng Sci Technol Int J (JESTECH) 37:101321

Feddes RA, Kowalik P, Kolinska-Malinka K, Zaradny H (1976) Simulation of field water uptake by plants using a soil water dependent root extraction function. J Hydrol 31(1–2):13–26

Findell KL, Berg A, Gentine P, Krasting JP, Lintner BR, Malyshev S, Santanello JA Jr, Shevliakova E (2017) The impact of anthropogenic land use and land cover change on regional climate extremes. Nat Commun 8(989):1–10

Gokmen M, Vekerdy Z, Verhoef W, Batelaan O (2013) Satellite-based analysis of recent trends in the ecohydrology of a semi-arid region. Hydrol Earth Syst Sci 17(10):3779–3794

Gupta H, Kling H, Yilmaz K, Martinez G (2009) Decomposition of the mean squared error and NSE performance criteria: implications for improving hydrological modelling. J Hydrol 377(1–2):80–91

Jarvis NJ (1989) A simple empirical model of root water uptake. J Hydrol 107(1–4):57–72

Jiongxin X (2005) The Water fluxes of the Yellow River to the Sea in the past 50 years, in response to Climate Change and Human activities. Environ Manage 35(5):620–631

KOP (2016) KOP Official Webpage: http://kop.gov.tr/. Accessed on 12 June 2023

Koycegiz C (2022) Impacts of land cover/land use change and relationship of water budget components in Konya Closed Basin: Historical research and future perspective. Konya Technical University PhD Thesis (In Turkish)

Koycegiz C, Sen OL, Buyukyildiz M (2023) An analysis of terrestrial water storage changes of a karstic, endorheic basin in central Anatolia, Turkey. Ecohydrology & Hydrobiology 23(4): 688-702

Lespinas F, Dastoor A, Fortin V (2018) Performance of the dynamically dimensioned search algorithm: influence of parameter initialization strategy when calibrating a physically based hydrological model. Hydrol Res 49(4):971–988

Long D, Chen X, Scanlon BR, Wada Y, Hong Y, Singh VP, Chen Y, Wang C, Han Z, Yang W (2016) Have GRACE satellites overestimated groundwater depletion in the Northwest India Aquifer? Sci Rep 6:24398

Nemati A, Najafabadi SHG, Joodaki G et al (2020) Spatiotemporal Drought characterization using gravity recovery and climate experiment (GRACE) in the Central Plateau Catchment of Iran. Environ Process 7:135–157

Rakovec O, Kumar R, Mai J, Cuntz M, Thober S, Zink M, Attinger S, Schäfer D, Schrön M, Samaniego L (2016) Multiscale and Multivariate Evaluation of Water Fluxes and States over European River basins. Am Meteorological Soc 17:287–307

Rodell M, Houser PR, Jambor U, Gottschalck J, Mitchell K, Meng CJ, Arsenault K, Cosgrove B, Radakovich J, Bosilovich M, Entin JK, Walker JP, Lohmann D, Toll D (2004) The Global Land Data Assimilation System. Bull Amer Meteor Soc 85:381–394

Rodell M, Famiglietti JS, Wiese DN, Reager JT, Beaudoing HK, Landerer FW, Lo MH (2018) Emerging trends in global freshwater availability. Nature 557:651–659

Rusli SR, Bense VF, Taufiq A, Weerts AH (2023) Quantifying basin-scale changes in groundwater storage using GRACE and one-way coupled hydrological and groundwater flow model in the data-scarce Bandung groundwater Basin, Indonesia. Groundw Sustainable Dev 22:100953

Samaniego L, Brenner J, Demirel MC et al (2018) The mesoscale hydrological model (mHM) documentation for version 5.9. Helmholtz Centre for Environmental Research-UFZ

Save H, Bettadpur S, Tapley BD (2016) High-resolution CSR GRACE RL05 mascons. JGR Solid Earth 121(10):7547–7569

Scanlon BR, Longuevergne L, Long D (2012) Ground referencing GRACE satellite estimates of groundwater storage changes in the California Central Valley, USA. Water Resour Res 48(4):W04520

Shen H, Leblanc M, Tweed S, Liu W (2015) Groundwater depletion in the Hai River Basin, China, from in situ and GRACE observations. Hydrol Sci J 60(4):671–687

Soni A, Seyd TH (2015) Diagnosing Land Water Storage Variations in Major Indian River basins using GRACE observations. Glob Planet Change 133:263–271

Tolson BA, Shoemaker CA (2007) Dynamically dimensioned search algorithm for computationally efficient Watershed Model Calibration. Water Resour Res 43(1):1–16

Tregoning P, McClusky S, Van Dijk A, Crosbie R, Pena Arancibia J (2012) Assessment of GRACE satellites for groundwater estimation in Australia. CSIRO Rep

TURKSTAT (2022) Turkish Statistical Institute Official Webpage. https://www.tuik.gov.tr/. Accessed on 23 January 2022

Wada Y, van Beek LP, Viviroli D, Dürr HH, Weingartner R, Bierkens MF (2011) Global monthly water stress: 2. Water demand and severity of water stress. Water Resour Res 47(7):1–17

Wada Y, van Beek LP, Wanders N, Bierkens MF (2013) Human water consumption intensifies hydrological drought worldwide. Environ Res Lett 8(034036):1–14

Wang J, Song C, Reager JT, Yao F, Famiglietti JS, Sheng Y, MacDonald GM, Brun F, Schmied HM, Marston RA, Wada Y (2018) Recent global decline in endorheic basin water storages. Nat Geosci 11:926–932

Wiese DN, Landerer FW, Watkins MM (2016) Quantifying and reducing leakage errors in the JPL RL05M GRACE mascon solution. Water Resour Res 52(9):7490–7502

Wu P, Christidis N, Stott P (2013) Anthropogenic impact on Earth's hydrological cycle. Nat Clim Change 3:807–810

Publisher's Note Springer Nature remains neutral with regard to jurisdictional claims in published maps and institutional affiliations.

Authors and Affiliations

Cihangir Koycegiz[1] · **Mehmet Cuneyd Demirel[2]** · **Omer Lutfi Sen[3]** · **Meral Buyukyildiz[1]**

✉ Cihangir Koycegiz
ckoycegiz@ktun.edu.tr

1   Department of Civil Engineering, Konya Technical University, Konya, Türkiye

2   Department of Civil Engineering, Istanbul Technical University, 34467 Istanbul, Türkiye

3   Eurasia Institute of Earth Sciences, Istanbul Technical University, Istanbul, Türkiye